

A MODEL FOR THE ORIENTATION OF LONG-TRACK SATELLITE STEREOPAIRS

Francelina A. Neto

Dept. of Photogrammetry and Surveying, University College London
Gower Street, London WC1E 6BT, England
ISPRS Commission IV

ABSTRACT

An orbital model for the orientation of long-track satellite linear array stereopairs is under development at University College London (UCL). The model is directed towards orientating images to be collected by future satellites such as ASTER (Advanced Spaceborne Thermal Emission and Reflection Radiometer) and QMI (Optical Mapping Instrument), expected to be launched in the late 1990s.

Results presented here were derived from simulated data since no satellite data is currently available. That used in the tests covers an area in south-east France, from which SPOT data was already available in the Department of Photogrammetry and Surveying (P&S). The results give indications as to the expected accuracy of this model.

Key Words: accuracy, aerotriangulation, mapping, space imagery

1. INTRODUCTION

The advent of SPOT in the late 1980s brought a new perspective into the study of cartography from space (Gugan et al, 1988; Dowman et al, 1988). SPOT is equipped with a pushbroom imaging system, with a nominal pixel size of 10 meters when operating in panchromatic mode (CNES, 1991), and high geometric accuracy. Its unrestricted commercial availability and high resolution made possible the use of SPOT data on an operational basis.

Several approaches to modelling SPOT imagery have been developed, and some of these models were described and compared during the OEEPE (Organisation Européenne d'Études de Photogrammétrie Experimental) test of 1989 (Dowman et al, 1991). Although SPOT is equipped with sensors measuring the attitude angular changes with time, which are provided with the image header file, this data was not used in the OEEPE tests. A comparison of the main findings by different centres, using the same 10 control points over the same area, is summarised in table 1.

Gugan et al, 1988, and Dowman et al, 1988, agreed that SPOT imagery may be suitable for both the production/revision of maps at scales up to 1:50,000 and the revision of some 1:25,000 scale maps. 3D (Three Dimensional) information is obtained using SPOT side-looking stereopairs (figure 1), though this type of imagery has some disadvantages. Firstly, the two images are taken at different times, usually separated by days or even months. Moreover, since the images are taken from different sides, with different illumination, identification of the points is more difficult. These effects may be reduced using along-track stereo imagery.

Research centre	rms of errors in (m)		
	H	Plan	3D
Hannover	6.4	13.5	14.9
IGN	4.7	8.7	9.8
Milan	11.5	16.5	20.7
Queensland	9.4	12.3	15.5
CCM	6.7	21.1	22.2
UCL	7.3	16.1	17.7

Table 1 - Precision obtained from orientating a common SPOT scene using different models (after Dowman et al, 1991)

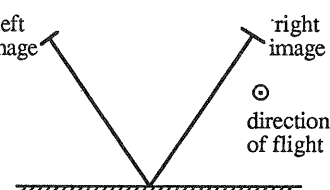


Figure 1 - Across-track stereo viewing

2. ALONG-TRACK STEREO SYSTEMS

Along-track camera systems have at least two optical systems simultaneously scanning the Earth's surface, each system having a different along-track angle. A stereoscopic image is obtained using backwards and forward-looking pairs of images as shown in figure 2. The cameras collect images within

seconds or minutes of each other, depending on the along-track angles. The orientation model may be simplified and the number of orientation parameters reduced, since the satellite orbit is common to both images. eg. ASTER & OMI.

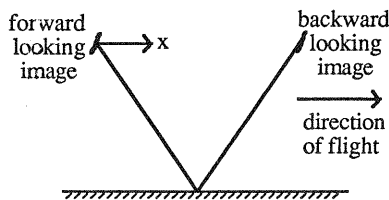


Figure 2 - Along-track stereo viewing

2.1. VNIR (Visible & Near Infrared Radiometer) on ASTER (Advanced Spaceborne Thermal Emission Radiometer)

The Japanese ASTER platform, will be carrying a 3 band Optical Sensor for Earth Observation (Arai, 1991). VNIR is a multispectral sensor covering visible and near infrared regions with a spatial resolution of 15m. The sensor will fly at an approximate altitude of 705 km imaging the Earth's surface with a 5,000 element linear CCD (Charged Coupled Device) sensor. This data is processed on-board, extracting 4,000 pixels from the full 5,000 pixels of imaged nadir and forward looking data. The forward looking sensor is set to a viewing angle of 29.7°, corresponding to a base to height ratio of approximately 0.6 (Arai, 1991).

2.2. OMI (Optical Mapping Instrument)

The OMI instrument is expected to be flown in the late 1990s at an orbital altitude of approximately 824 km and inclination of 98.7°. The baseline OMI design is for two views, one 20° forward off nadir and the other 20° backwards. For a total coverage of the Earth's surface in a minimum time, an across-track capability of ±20° will be introduced. The base to height ratio of the system is approximately 0.7. The sensor is composed of two 12,000 CCD linear arrays, with a 5m ground resolution (British Aerospace, 1991).

2.3. OPS (OPtical Sensor) on JERS-1 (Japanese Earth Resources Satellite-1)

The OPS is an electronic scan typed optical sensor to be flown on the JERS-1 System. The JERS-1 orbit is a sun synchronous orbit at 568 km height, with orbital inclination 97.7°. The sensor has a 4,096 CCD linear array with a 18.3 m range resolution, and 24.2 m resolution in azimuth. The stereo capability is obtained by a nadir and a 15.3° forward imaging sensor, with a base to height ratio of approximately 0.3 (MITI/NASDA, 1990).

3. MODEL DESCRIPTION

Due to its dynamic nature, linear imagery has a distorted

multiple plane perspective, and is unable to be orientated as a stereomodel obtained from two frame photographs. From previous studies carried out on SPOT data, it was concluded that the best models were obtained using the orbital parameters for the orientation plus the image header file. This approach also has the advantage of minimizing the ground control data needed. Consequently, the following orbital method was adopted for the orientation of along-track stereo imagery.

The geocentric coordinate system was adopted to avoid problems of map projection discontinuities, as well as to reduce the number of formulae, and hence run time. For continuity, the position of the sensor in space is also described in geocentric coordinates (X_S, Y_S, Z_S), which can be computed for each image line. The image coordinates system (x, y, z) is such that x is the number of lines in the image along the direction of flight, y is the number of samples in the across-track direction, and z is the principal distance of the camera, perpendicular to the image (Figure 3). The only measurement of time available is x , which is used to describe time-orientation relationships. However, since the image is linear, x is assigned to zero, while z always takes the value $-f$, where f is the principal distance of the camera.

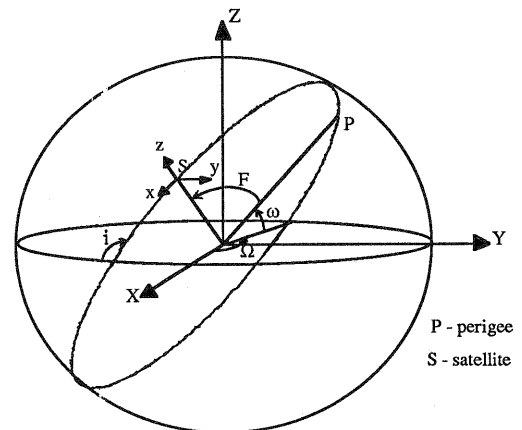


Figure 3 - Orbital parameters and geocentric system

The algorithm uses Eulerian parameters ($a, e, i, \Omega, \omega, F$) to fix the position of the satellite in space (figure 3) where a is the semi-major axis, e the eccentricity, i the inclination, Ω the longitude, w the argument of perigee and F is the true anomaly of the orbit. The elliptical orbit is modelled (using these parameters) using the rotation matrix R_0 (Equations 1 to 4).

$$R_0 = R_F \cdot R_i \cdot R_\Omega \quad (1)$$

$$X_S = R_0^T \cdot D \quad (2)$$

$$D = (0, 0, r)^T \quad (3)$$

$$r = a (1 - e^2) / (1 - e \cdot \cos F) \quad (4)$$

where

$$\begin{aligned} F' &= (F + \omega) - 90^\circ \\ i' &= 90^\circ - i \\ \Omega' &= \Omega - 180^\circ \end{aligned}$$

The major components of dynamical motion are the Earth's rotation and the satellite movements along the orbit path. These motions have been modelled as linear angular changes of F and Ω with time, for which the second degree zonal component J_2 of the Earth gravitational potential is the principal component. The first order perturbations caused by J_2 and the Earth's rotation is given by equations 5, 6 and 7 (Kaula, 1966).

$$\Omega' = -\frac{3}{2} \cdot \frac{J_2 \cdot n \cdot R_e^2}{a^2 \cdot (1-e^2)} \cdot \cos(i) + v \quad (5)$$

$$w' = -\frac{3}{4} \cdot \frac{J_2 \cdot n \cdot R_e^2}{a^2 \cdot (1-e^2)} \cdot [1 - 5 \cdot \cos^2(i)] \quad (6)$$

$$M' = \frac{3 \cdot J_2 \cdot n \cdot R_e^2 \cdot (3 \cos^2(i) - 1)}{4 \cdot a^2 \cdot (1-e^2)^{3/2}} \quad (7)$$

where R_e is the Earth's semi-major axis, v is the Earth rotation and n is the mean motion of the satellite. M is the mean anomaly and M' is its variation with time, from which the value of F can be calculated.

Since the satellite is not pointing precisely towards the centre of the Earth, additional attitude rotations are introduced by an orthogonal matrix R_A , which characterizes the effects of pitch, roll and yaw, and their variations with time. The viewing angle also varies for each image and the effect of its geometry is added to the formulae as another orthogonal matrix R_m .

The collinearity equations (8a and 8b) are used for the orientation of a single image, where u_{ij} are the elements of matrix U (Equation 9), X_A, Y_A, Z_A are the geocentric coordinates of each control point and s is a scale factor.

$$\left\{ \begin{array}{l} -z \cdot \frac{u_{11}(X_A - X_S) + u_{12}(Y_A - Y_S) + u_{13}(Z_A - Z_S)}{u_{31}(X_A - X_S) + u_{32}(Y_A - Y_S) + u_{33}(Z_A - Z_S)} = 0 \\ y - z \cdot \frac{u_{21}(X_A - X_S) + u_{22}(Y_A - Y_S) + u_{23}(Z_A - Z_S)}{u_{31}(X_A - X_S) + u_{32}(Y_A - Y_S) + u_{33}(Z_A - Z_S)} = 0 \end{array} \right. \quad (8a) \quad (8b)$$

$$U = \frac{1}{s} R_m R_A R_0 \quad (9)$$

Since along-track stereopairs are taken during the same orbit, with a short time interval in between, the method described above may be advantageously modified. However, an additional parameter is required, namely a variable to represent the time displacement, Δt . Hence if the first image is arbitrary chosen, Δt sets the position of the second image relative to the first, as shown in figures 4a and 4b.

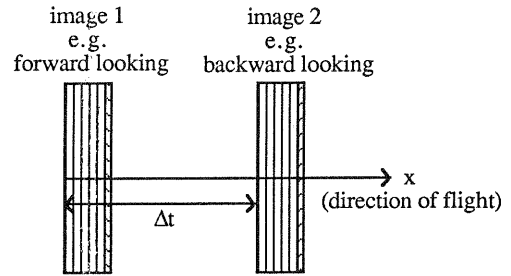


Figure 4a - Time displacement Δt between two images taken during the same orbit (represented on the image).

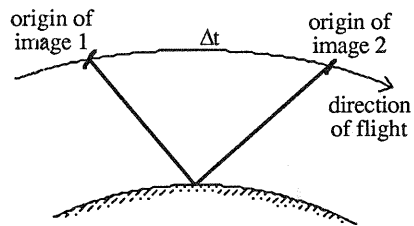


Figure 4b - Time displacement Δt between two images taken during the same orbit (orbit representation).

The two images of an along-track stereopair are taken during a common orbit, being the values for semi-major axis, inclination, longitude of the ascending node and argument of perigee the same for the two images. If the origin of the first image is taken as origin of the second image, the values of the other orientation parameters are also common to both images, as they are set for the origin. However, the points are identified in the second image by their line and sample values, and the line number being a measurement of time on the second image is not related to the origin of the first image. The time displacement Δt acts as the translation in time suffered by the second image relative to the first, so that the orientation parameters for each line of the second image are affected by the line position x (measurement of time) plus Δt . The orientation parameters for each position become then dependent on Δt and correlation occurs.

In all $10+n$ parameters are used, 10 to orientate the strip, and n time displacement parameters for the $n+1$ images. The 10 parameters used to orientate the strip are the semi-major axis, the true anomaly, the longitude of ascending node, the orbit inclination, and six more parameters defining the attitude of the sensor with time. The argument of perigee was considered nil in the computations because the orbit eccentricity is very small in the cases considered (< 0.002) and its effect on the model orientation can be expressed by the effect of the true anomaly. An attitude model is initially formed using the attitude data file provided and the attitude parameters used in the iterative process adjust this attitude model to the ground control.

An along-track stereopair can be orientated using as few as 3 control points per image, providing 12 observation equations, for the 11 parameter solution. The number of control points may be decreased if a poorer orientation is adopted, for example when 2 control points per image are used, then a 7 parameter orientation is possible with some redundancy.

It has been shown (O'Neill et al, 1989) that better results may be obtained if on-board recorded information is used. The algorithm automatically takes an *a priori* precision of the measurements, the control used in the orientation plus information recorded during flight. Initial information of the start values is used to form a weighting matrix. Currently, the algorithm implemented uses information in an auxiliary data file with additional information being provided by the user.

4. SIMULATED DATA

Tests in order to study the precision of the orbital model described above were performed. The data used was simulated since no satellite along-track stereo data is presently available. Two sets of SPOT data covering a region in south-east France (about 200 per 600 km), available at UCL(P&S) (Veillet, 1991), were used to calculate the orbital parameters of a vertical theoretical SPOT-like orbit.

The simulated image coordinates of 106 ground points were computed using equation 10 and their known geocentric coordinates. The iterative process was run for two different along-track viewing angles, terminating when a correction smaller than 0.001mm was encountered for $x=0$ (this correlates to an error smaller than 0.1 line/sample).

$$\begin{bmatrix} x \\ y \\ -f \end{bmatrix} = \frac{1}{s} \cdot R_m R_A R_0 \begin{bmatrix} X_A - X_S \\ Y_A - Y_S \\ Z_A - Z_S \end{bmatrix} \quad (10)$$

A first set of images simulate backward and forward angles of 26°, emulating a SPOT-like along-track stereopair with a base to height ratio of approximately 1. A second simulation calculated both ASTER-like, OMI and OPS sensor data. All simulations used Westin's variogram (Westin, 1991), which models the variation of the attitude parameters with time. A pseudo-error with standard deviation 0.5 line/sample was added to the simulated data, as an average error of half a pixel of identification in the points on the image may be assumed.

In the OEEPI tests (Dowman et al, 1991) it was concluded that the results underwent only small variations when more than six control points were used in the orientation. Hence, six points were chosen from the simulated data for ground control, the other one hundred points being used for checking purposes.

5. RESULTS OF TESTS

The scenes were orientated using the control configuration shown in figure 5, with the control distribution of the terrain

being chosen such that it would cover all types of relief possible and would be well distributed for better orientation.

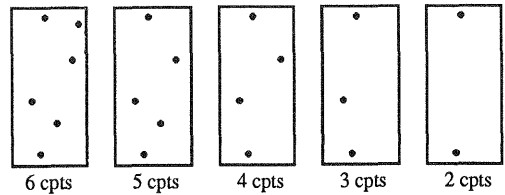


Figure 5 - Control configuration used in the tests

The same configuration was used to orientate the different sets of simulated data. The root mean square(rms) of the errors obtained with the check data are presented in tables 2, 3, 4 and 5. The 2 control points models were run using only 7 orientation parameters, plus Δt . The only attitude parameter variation with time considered in the computation was that of pitch due to its larger effect on height, and the bias in roll being fixed using the attitude file information. The models respective precisions were evaluated by comparing the UTM (Universal Transverse Mercator) coordinates calculated after orientation, to the known simulated coordinates of the 100 check points not used in the model processing.

The precisions obtained using the SPOT-like along-track stereopair (10 m pixel resolution) are given in table 2. Analogous results for the ASTER (15 m pixel resolution), OMI (5 m pixel resolution) and OPS (18.3x24.1 m pixel resolution) are given in tables 3, 4 and 5 respectively.

Number of control points	rms of errors found in UTM (m)			
	E	N	H	3 D
6	5.2	5.3	5.9	9.5
5	7.0	6.5	7.6	12.2
4	7.0	6.5	7.6	12.2
3	8.7	5.1	9.4	13.8
2	10.1	6.7	8.8	15.0

Table 2 - Precision obtained for a SPOT-like simulated orbit with along-track stereo viewing (10m pixel resolution).

Number of control points	rms of errors found in UTM (m)			
	E	N	H	3 D
6	7.9	8.6	19.6	22.8
5	9.1	10.4	17.8	22.5
4	9.1	10.4	17.8	22.5
3	7.3	14.2	19.4	23.4
2	6.9	6.7	24.5	29.1

Table 3 - Precision obtained using ASTER simulated data (15m pixel resolution).

Number of control points	rms of errors found in UTM (m)			
	E	N	H	3 D
6	3.0	2.7	5.7	7.0
5	3.0	3.0	6.0	7.3
4	2.8	3.4	6.6	7.9
3	2.9	2.6	7.1	8.1
2	2.1	2.4	8.6	9.1

Table 4 - Precision obtained using OMI simulated data (5m pixel resolution).

Number of control points	rms of errors found in UTM (m)			
	E	N	H	3 D
6	9.4	11.5	44.9	47.3
5	10.2	10.7	47.2	49.4
4	10.3	10.8	47.6	49.5
3	10.4	11.7	50.0	50.4
2	13.3	16.3	65.8	69.1

Table 5 - Precision obtained using OPS simulated data (18.3x24.2 m pixel resolution).

6. ANALYSIS OF THE RESULTS

The major orientation problem of along-track stereopairs is the effect of relief in the image producing a parallax in the flight direction, correlated to the effect of pitch. Since a one-orbit algorithm for the pair is being considered, there is an additional problem of correlation between the time displacement Δt and the pitch. These correlations are balanced using a weighting matrix of the orientation parameters. Despite these problems, the approach has the major advantage of minimizing the number of parameters needed, and hence the control and run time of the algorithm.

Using the initial data set, the precision of some orientation parameters is initially evaluated. In conjunction with other information, either entered by the user or set for the sensor whose image is being used, an *a priori* weighting matrix is formed considering all parameters independent. This procedure keeps the solution within acceptable limits, conditioned by the initial assumption of precision. Otherwise, the correlation between some of the parameters would prevent the solution from converging, as big variations during the iterative process might occur. Although the independence between the orientation parameters is currently being assumed, this is known to be false. In practice, there is a dependence between the orientation parameters and the resulting weighting matrix should not be a diagonal matrix as it was assumed during these tests.

Decreasing the number of control points to 4 (as identified in both images) does not significantly influence the results. However, the use of only 3 or 2 control points in the orientation

process produces lower precision models, characterized by a worsening in the height precision. With the exception of the SPOT-like along-track pair, the height precision was always larger than the pixel resolution. This is justified by the larger base to height ratio of the former, approximately 1, than the respective 0.6, 0.7 and 0.3 of the ASTER, OMI and OPS sensors, which worsen the correlation between the effects of the terrain relief and pitch.

The precision of planimetric positioning is in all cases approximately of the same order of the pixel ground resolution, for a 3 to 4 control points model. Sub pixel planimetric precision may be obtained with a 6 control points orientation, considering a half a pixel precision in the identification of the control. Experimentally, it is known that base to height ratios smaller than 0.5 give very poor heighting accuracy. This was confirmed once more in the tests carried out with the OPS sensor data. The pixel resolution of the OPS sensor (18.3x24.2 m) was the worse of all the four sets of data considered, and a smaller precision was expected from modelling this data. Moreover, a very poor height resolution was found. While for the tests carried out with the other sensors the worse errors found in height were smaller than twice the pixel resolution, for the OPS data the smallest error found was approximately twice the pixel resolution of the sensor.

Although the errors found in height were worse than in planimetry for the data sets whose base to height ratios were bigger than 0.5, they were still below twice the pixel resolution of the sensor, in the worse models (2 control points). Better models were obtained using 6 to 4 control points, with height accuracy of the same order of the pixel resolution. The 3D vector error was found to be larger than the pixel ground resolution in all the studies carried out.

Comparing the results obtained in these tests (table 2) with the previous studies with SPOT data (table 1), the poorer precision obtained in height from along-track stereo imagery, due to the correlations mentioned previously in this paper, is confirmed. OMI results are better than the other along-track models because OMI pixel resolution is also better than any of the other sensors.

7. CONCLUDING REMARKS

Further developments to the algorithm are under investigation for possible improvements to the model such as the correlations between the orientation parameters which lead to poor height accuracy. The use of a more precise and real weighting matrix for minimisation of correlation between the orientation parameters is under study. The algorithm is also being adapted to accommodate stereotriangulation, to consider simultaneously stereo images from several sensors, and to take in account a quality factor linked to the measurements.

It is also being revised the use of conjugate points in the modelling process, in order to decrease the number of control needed. However, from previous studies carried out in this area, high instabilities occur during the iterative process, mainly

affecting the height precision of the model. The solution to this problem also lays in a possible improvement of the weighting matrix of the orientation parameters, to stabilize the solution.

8. REFERENCES

1. Arai, K., 1991. An assessment of height estimation accuracy with EOS-a/ASTER Data. Proceedings of Spatial Data 2000. Oxford. Remote Sensing Society. pp 73-75.
2. British Aerospace (Space Systems) Limited, 1991. The OMI Programme. Technical Information. 4 pages.
3. CNES, 1991. SPOT User's Handbook. SPOT Image. France.
4. Dowman, I.J. and Peacegood, G., 1989. Information Content of High Resolution Satellite Imagery. *Photogrammetria*, 43 (6): 295-310.
5. Dowman, I.J., Neto, F. and Veillet, I., 1991. Description of test and summary of results. Test of triangulation of SPOT data. OEEPE Official Publication No 26.
6. Gugan, D.J. and Dowman, I.J., 1988. Accuracy and Completeness of Topographic Mapping from SPOT Imagery. *Photogrammetric Record*, 12 (72): 787-796.
7. Kaula, W.M., 1966. Theory of Satellite Geodesy. Blaisdell, Waltham, Mass.
8. MITI/NASDA (Ministry of International Trade and Industry/National Space Development Agency of Japan), 1990. Outline of the JERS-1 System. Japan. 31 pages.
9. O'Neill, M.A., and Dowman, I.J., 1991. A New Model for Orientation of SPOT Data. OEEPE Official Publication No 26.
10. Veillet, I., 1991. Background to test on Triangulation of SPOT Data. OEEPE Official Publication No 26.
11. Westin, T., 1991. Empirical Models for Attitude Variability of the SPOT 1 Satellite. *Photogrammetric Record*, 13 (78): 917-922.

ACKNOWLEDGEMENTS

I am thankful to the Calouste Gulbenkian Foundation for sponsoring me, to my supervisor Professor I.J.Dowman (UCL), for his support to this study, and to Antony Richards for proof reading this paper .